LAASP 100-m Antenna Wind Performance Studies

R. Levy and M. S. Katow
DSN Engineering Section

Structural design procedures are described for the LAASP antenna system to meet performance requirements under gravity and wind loading. A computational method is shown for the evaluation of performance in response to wind loading. Cumulative probability distribution curves for wind loading gain reductions for 100-m-diameter antennas are developed to compare a relatively heavy baseline reflector backup structure with two lighter-weight structures; all have equivalent, acceptable performance for gravity loading.

I. Introduction

Design studies for the Large Antenna Station Project (LAASP) paraboloidal antenna structures are undertaken to derive cost and performance tradeoffs associated with a number of configuration alternatives. Both cost and performance can be characterized by any of a number of quantitative measures, while configuration alternatives also are conceptually limitless. Consequently, to expedite timely completion of any study, some restrictions on the scope are essential. Nevertheless, within a framework of practical and reasonable restrictions, it is feasible to develop significant parametric study information for a comprehensive range of antenna structure designs within a given diameter class.

Within the context of the present discussion, cost will be measured by the structure weight. It is well known that weight is an imperfect measure of structure cost when a wide variety of configurations with diverse fabrication, material, and installation requirements are contemplated. However, when alternative configurations are similar in concept, structure weight is a convenient and acceptable cost measure. Performance will be measured by the antenna radio frequency (RF) gain reduction, which depends upon the structural deformations caused by gravity and wind loading.

Gravity loading, which is always present on antenna structures, is deterministic and well understood. Wind loading is statistical, and the assessment of related response is more complex. Depending upon the location, wind can have a significant effect upon performance. Other loadings such as thermal, shock, and earthquake are primarily stochastic, difficult to quantify, and of relatively short duration. These loadings can be treated as constraints on the design to maintain structure integrity and survivability but are not included for evaluation of operating performance.

Configuration studies will be limited to be within one particular reflector class: The traditional structural format of radial rib trusses braced by circumferential hoop ring trusses. Within this format class, nevertheless, there are many possible variations of the geometrical arrangement, such as proportions, numbers and spacing of trusses, and the configuration of the external supporting structures. Several of these variations are

examined early in the present study but, for brevity, the designs to be described here will include only the preferential geometry as previously developed.

Here the emphasis will be placed upon the relationships between weight and performance for wind loading. The calculational procedure and results obtained will be described for a proposed 100-m-diameter antenna reflector system illustrated in Fig. 1. This system is intended to operate at the X-band frequency of 8.5 GHz. Cumulative probability distribution curves of gain reduction for wind loading will be shown for three alternative reflector designs for this system. These designs have the same geometry and differ only in the cross sectional areas of the bars chosen for the reflector backup structure. They represent a baseline design and two lighter variations with weight reductions of up to 30%. All three designs are constrained to have equivalent performance in the absence of wind loading. The maximum gain reduction due to gravity loading is less than 10% of the total gain reduction from all sources. Those consist of manufacturing and surface alignment errors and subreflector and quadripod blockage.

II. Sources of Gain Reduction

Table 1 is a summary of the sources of gain reduction that have been considered for gravity or wind loading. Two categories are identified: the deformation-type category includes pathlength phase errors of the radiofrequency (RF) beam; the beam-deformation-type category covers pointing misalignment losses of the main beam with respect to the target.

Referring to the table, backup structure contribution is computed with respect to the paraboloid that best fits the deflected surface. Surface panel contributions are also considered with respect to a best-fitting surface. The subreflector offsets are the axial and lateral mismatches of the subreflector position from the focal point of the best-fitting paraboloid. For computational purposes, these offsets can be converted to equivalent additional backup structure deformations (Ref. 1). For gravity loading, which is repeatable and calibratable, the subreflector can be repositioned to the actual focal point, and thus the offsets produce no gain reduction. Subreflector surface deflections are another source of deformation-type losses. However, these will be disregarded because appropriate design can make them small.

The wind speeds are represented by the conventional model of a slowly varying, quasi-steady component and a superimposed gust turbulence. Beam deviation error that results from the steady component of the wind speed is corrected by a programmed pattern search that removes these low-frequency pointing errors. We make a conservative assumption, however, that the pattern search is too slow to overcome the gust effects, so that gust loading always produces gain reductions through beam deviations. The pointing errors from gravity loading can be overcome by calibration that compensates the input command signal. The servo loop error occurs because the servo system is not fully effective in compensating for the higher-frequency components of the gust disturbance torque. The ability of the servo system to compensate depends upon the servo loop transfer function in conjunction with the wind gust spectrum. Calculations for typical antenna systems show that from 75% to 90% of the angular errors detected at the encoders can be removed by compensation. To be conservative, calculations here assume compensation of only 75% of these error magnitudes.

III. Reflector Design Synthesis

The baseline reflector backup structure design was developed by an evolutionary process. Although the JPL-IDEAS computer program (Ref. 2) was used as a pivotal design tool to perform analysis and optimization of member cross-sectional area selection, no software was available to optimize the geometrical proportions for this structure. Consequently these proportions were developed from a sequence of trial variations of the geometry. The variations were tested by analysis and member area redesign within the IDEAS program to assess their ultimate potential.

The ordinarily laborious and time-consuming task of preparing the extensive data card sets required for structural computer analysis was expedited by a program that automatically generated these cards for each variation. This program supplies almost all of the card images needed to describe reflector backup structures of the conventional radial rib truss and circumferential hoop type of construction. The sequence of trial geometry generation and subsequent testing entails generation and processing of an extensive data bank; nevertheless, it is executed rapidly. Furthermore, only a limited amount of effort by the engineer is needed. His participation is required primarily for decision-making to guide the operations and to select from among the many options available to him, with only a small requirement for time to be spent on clerical tasks.

The root mean square (rms) pathlength deviation of the reflector surface from the best-fitting paraboloid was selected as the performance measure for design evaluation. The goal was to achieve a reasonable balance between response to gravity loading and response to wind loading. For the gravity loading, the objective response was the average of the rms values over the elevation angle range weighted by tracking mission probabilities (Ref. 3) associated with the elevation angles. A criterion wind-loading case was established to represent the condition of the antenna at the 60-deg elevation angle

with a rear wind at an arbitrary reference speed of 13.4 m/sec (30 mph). Previous experience with similar antennas indicated that this wind orientation was likely to be the most severe. During all of the redesign iterations, member area selections were subjected to constraints on stress and buckling for the gravity loading, for the criterion wind loading, and for additional wind loadings that represented the most severe operational wind (31.3 m/sec) and the survival wind (44.7 m/sec).

The geometry evolved for the baseline design resulted in a nearly homologous response (Ref. 4) for gravity loading and a very good surface rms (0.69 mm) for the criterion wind loading. Two lighter-weight variations of the basic design were developed by permitting a degeneration of performance for the criterion wind loading but at the same time retaining the stress and buckling constraints for all loads and by invoking a new constraint that maintained the performance for the gravity loading. The weight of the backup structure and counterweight for the baseline design was 1210 tons, and the lighter designs produced reductions of 200 and 335 tons with the wind criterion loading rms values of 0.86 mm and 0.93 mm respectively.

The alidade comprises a much less complex analytical model than the reflector. The few data cards required for analysis and redesign were hand-generated. The final geometry also entailed evolutionary proportioning to achieve a favorable arrangement. Analysis and member redesign were performed by the IDEAS program using an option invoked to maximize stiffness with respect to pointing accuracy for wind loading. Only one alidade design was developed, and this is used to support all three of the backup structures.

The alidade model was eventually converted for analysis by the NASTRAN program (Ref. 5). This was done for the convenience of having a direct output of specific internal rotation angles related to the servo loop wind gust error. The NASTRAN program analysis included the bending stiffness of the alidade bars, which is presently not possible within the IDEAS program. Nevertheless, responses from the two programs agreed closely, indicating that the bending rigidity is not significant.

IV. Computational Model for Wind Loading Gain Reduction

A multidimensional four-component statistical model was used for computation of gain reduction due to wind loading. The four random components were (1) V, the mean wind speed; (2) v, a superimposed gust turbulence; (3) AZ, the azimuth of the wind relative to the antenna pointing direction; (4) EL, the elevation of the antenna relative to the horizon.

The mean speed has slow variations that comprise periodic components measured by hours or days. Statistics of the mean speed obtained for the same site (Goldstone, California) as the proposed 100-m antenna have been tabulated in Ref. 6.

The gust speed was described by the conventional model, which represents the gusts as gaussian, with zero mean and standard deviation σ_v proportional to the mean speed; e.g.,

$$\sigma_v = CV \tag{1}$$

The tabulated mean speeds are based upon observations at a 46-m (150-ft) height above ground. For convenience, the mean speeds here are also considered at the same height. Estimating the surface drag coefficient at 0.006 for the proposed terrain and using the computed power law coefficient for speed variations with height equal to 0.1405 (Ref. 6), we find $C = 0.1533$.

Gusts are the dynamic component of the wind speed. Spectral decompositions according to conventional models (Refs. 7, 8) show that the predominant fluctuations are characterized by periods in the order of several seconds to minutes. The natural frequency of the antenna-reflector system of Fig. 1 will be at least 1 Hz for the slowest natural mode. The response of such a system to both the mean speed and the gust speed is essentially the same as for static load application. Consequently the structural response can be computed as a static response to total wind loading $\underline{V}$ where

$$\underline{V} = V + v \tag{2}$$

Wind tunnel test data on antenna reflector and alidade components (Refs. 9, 10) were used to convert from wind speeds to pressure loadings on the proposed reflector and alidade structures. Wind tunnel tests are a logical and reasonable basis for deriving the pressures and forces for the mean components of the wind speeds. Nevertheless, it is recognized that using the same type of conversion for gust effects is a major assumption and simplification of this model. The gust speeds actually have a three-dimensional spatial correlation for which theoretical models require further development. A possible approach to providing a better estimate of the gust loading is available through computer simulation (Ref. 11). However, it was estimated that the application of this approach would have entailed a major additional computational effort and also more wind tunnel test data than is currently available. Nevertheless, despite the simplified representation for gust loading, the present work employs the same formulation to compare alternative designs and should furnish a reasonable basis for comparison.

The distribution of wind azimuths relative to the antenna was also simplified in this model by assuming a uniform distribution in the range of azimuths from 0 to 360 deg. Because of symmetry, only half of this range is considered in the calculations. Had statistics been availabe to describe the distribution of wind azimuths at the proposed site, it would have been possible to determine a more accurate distribution of relative wind azimuths in conjunction with analysis of the statistics of proposed antenna targets. The related uncertainty in the assumption of uniform relative azimuths does not appear to be sufficient to undertake the additional computational complexity.

The distribution of antenna elevations was considered for elevations in the range of 0 to 90 degrees. Probability densities of the elevation angles were available from analysis of composite statistics of planetary tracking missions (Ref. 3).

For computational purposes, discretization of the four random components into specific class marks and class intervals was as follows:

1. Mean speed, V; 0 to 22.35 m/sec (50 mph) at intervals of 2.235 m/sec (5.0 mph). 10 terms.
2. Gust speed, v; -4 to +4 standard deviations. 19 terms unevenly spaced with finest resolution in the vicinity of 0 standard deviations.
3. Relative azimuth, AZ; 0, 30, 60, 90, 120, 150, 180 deg. 7 terms.
4. Antenna elevation, El; 0, 30, 60, 90 deg. 4 terms.

The computational results are represented by cumulative probability distributions of gain reduction. The distributions cover the range of 0 to 4 decibels (dB) at 100 discrete increments of 0.04 dB. Conditional distributions (10 X 7 X 4 = 280) were developed for each combination of mean speed (including the related gust probability), azimuth, and elevation angle. The final distributions were the composite of the conditional distributions weighted by the probability associated with the mean speed, azimuth, and elevation class marks. This very simple method of combining the conditional distributions is permissible from the assumption of independence of wind speed, azimuth, and elevation angles.

V. Computation of Gain Reduction Distribution

The computational method used to compute a typical gain reduction conditional probability distribution will be described here. Each of these distributions represents the random effects of wind gusts and is conditioned upon specific values of mean wind speed, wind azimuth, and antenna elevation.

With reference to gain reduction categories A and B of Table 1, the wind pressures, and consequently the forces, are proportional to the square of the wind speed. The deformations and deviations (pointing angle errors) are proportional to the forces. Gain reductions for category A are proportional to the squares of the deformation. Gain reductions for category B are proportional to the squares of the differences in deviations for the total wind speed minus the deviations for the mean wind. Consequently the gain reductions for these two categories can be represented as

$$G_A = G_R(\underline{V}/V_0)^4 \tag{3}$$

$$G_B = G_P(\underline{V}^2 - V^2)^2/V_0^4 \tag{4}$$

in which

G_A, G_B = category A, B, gain reduction

V_0 = reference mean wind speed

$\underline{V}$ = total (mean + gust) speed

V = mean speed

G_R = category A gain reduction at reference speed

G_P = category B gain reduction computed for V_0 and not allowing correction for the mean speed. Thus G_P is equivalent to a "blind pointing" loss for V_0.

To obtain a convenient computational formula, the gust speed v is replaced by a standardized normal variate Z such that

$$Z = v/\sigma_v \tag{5}$$

Then from Eq. 1

$$v = CZV \tag{6}$$

and from Eq. 2

$$\underline{V} = V(1 + CZ) \tag{7}$$

From these relationships, Eqs. 3 and 4 can be combined so that the total gain reduction G_T, which is the sum of G_A and G_B, can be expressed as

$$G_T = (G_R f_R + G_P f_P) \cdot (V/V_0)^4 \tag{8}$$

where

$$f_R = 1 + 4\,CZ + 6(CZ)^2 + 4(CZ)^3 + (CZ)^4 \tag{9}$$

$$f_P = 4(CZ)^2 + 4(CZ)^3 + (CZ)^4 \tag{10}$$

The conditional distribution for gain reduction, $F(G_T)$, can then be obtained from Eq. 8, using the relationships of Eqs. 9 and 10. Although the procedure is automated within a digital computer program, equivalent operations can be illustrated graphically with respect to Fig. 2 as follows:

① Compute G_T for a set of values of Z in the range (-4, +4) and plot G_T vs Z, as in Fig. 2a.

② At a selected value of gain reduction G_{Ti}, find the intersections of G_{Ti} with the curve in ①.

③, ④ Project the intersections down to the curve in Fig. 2b. This curve is constructed to be the standard normal cumulative probability distribution of Z. Read the ordinates where the projections intersect the curve.

⑤ The value of the distribution of gain reduction at G_{Ti} is the difference in the ordinates read from the curve of Fig. 2b.

VI. Computational Procedure

Figure 3 contains a schematic diagram of the complete computational procedures used to derive the gain reduction distribution for wind loading. The following notes apply to the labeled blocks of the figure:

Block 1. Wind tunnel pressure distribution data for specific relative wind attitudes with respect to the antenna are converted to the force data required as input for reflector analysis. The forces are represented by the three Cartesian coordinates at each node and are derived from the interpolated wind pressures, the surface area tributary to the node, and the components of the unit vector normal to the surface. Development of force data, except for the interpolation, is automated. Wind loading on the structural members of the alidade is also developed from wind tunnel data. For both reflector and alidade, sets of loads are developed to correspond with the discretization of wind azimuth and antenna elevation.

Block 2. The reflector is analyzed by the IDEAS program to supply the responses to the wind loadings. The program is used here for analysis only, by specifying no redesign cycles.

Block 3. The alidade is analyzed by the NASTRAN program to find the response for the wind loadings. Wind reactions of the reflector on the alidade are included.

Block 4. Computation of pathlength deviations from the best-fitting paraboloid are automated within IDEAS.

Block 5. Gain reductions for subreflector offsets are calculated by hand, using results from the reflector analysis.

Block 6. Reflector contributions to the pointing errors are automated within a separate computer program. Results are assembled within a matrix (4 elevations × 7 azimuths).

Block 7. Alidade contributions to pointing error and to servo loop are hand-computed (presently) and assembled within matrices.

Block 8. The category A (deformation-type) gain reductions are combined by hand calculation. These individual G_R terms (Eq. 3) are assembled within a matrix.

Block 9. A compute program derives a matrix containing the G_P terms (Eq. 4). In the preceding blocks, the alidade and reflector pointing deviations have been computed with separate components for the elevation and cross-elevation axes. Vector addition is required to combine the separate components.

Block 10. The G_R and G_P matrices are input. A computer program develops conditional distributions for gain loss, described previously, for all 280 combinations of mean wind speed, wind azimuth, and antenna elevation.

Block 11. The computer program of Block 10 applies probability weighting factors for mean speed, wind azimuth, and antenna elevation to the conditional distributions and assembles the composite distribution of gain reduction for wind loading.

VII. Results and Conclusions

Figure 4 shows the distribution of gain reduction for wind loading for the baseline 100-m antenna system and the

two alternative designs with lighter reflector backup structures. As stated previously, all designs provide equivalent high performance for gravity loading.

For ready reference, Fig. 4 tabulates reductions at a few selected percentiles of the distribution. It can be noted, for example, that the reduction in weight of 335 tons for the lightest structure is achieved with a reduction in performance of 0.37 dB (8% loss in efficiency) at the 98th percentile, and with much smaller reduction at lower percentiles. On the average, the table shows this design to be only 0.04 dB worse than the baseline.

Whether or not the lightest design shown, or possibly a design lighter than any of these, will be adopted must be considered in view of the performance requirements for the entire system. Tracking mission requirements and desired reliability in conjunction with other sources of gain reduction must be integrated within this type of evaluation.

References

1. Katow, M. S., "Evaluating Computed Distortions of Parabolic Reflectors," *Mechanical Engineering in Radar Symposium,* Nov. 8-10, 1977, Washington D.C.
2. Levy, R., "Computer-Aided Design of Antenna Structures and Components," *Computers and Structures,* Vol. 6, pp. 419-428, Pergamon Press, 1976.
3. Levy. R., "Antenna Bias Rigging for Performance Objective," *Mechanical Engineering in Radar Symposium,* Nov. 8-10, 1977, Washington D.C.
4. Von Hoerner, S. "Homologous Deformations of Tiltable Telescopes," *J. Struct Div., Proc. ASCE 93(ST-5),* Proc. Paper 5529, pp. 461-485.
5. *The NASTRAN User's Manual,* NASA SP-222(01), C. W. McCormick, editor, May 1973.
6. Levy, R., and McGinness, H., *Wind Power Prediction Models, JPL TM 33-802,* Jet Propulsion Laboratory, Pasadena, California, Nov. 1976.
7. Davenport, A. G., "The Spectrum of Horizontal Gustiness Near the Ground in High Winds," *Quarterly Journal of the Royal Meteorological Society, London, Vol. 87, Aug. 1961, pp. 194-211.*
8. Hino, M., "Spectrum of Gusty Wind," *Proceedings of the Third Conference on Wind Effects on Buildings and Structures,* Tokyo, Japan, Sept. 6-11, 1971, pp. 69-78.
9. Fox, N. L., *Load Distributions on the Surface of Paraboloidal Reflector Antennas,* Internal Memorandum JPL-CP 4, Jet Propulsion Laboratory, Pasadena, California, July 1962 (JPL internal document).
10. Blaylock, R. B., *Aerodynamic Coefficients for "A Model of A Paraboloidal-Reflector,"* Internal Memorandum JPL-CP6, Jet Propulsion Laboratory, Pasadena, California, May 1964 (JPL internal document).
11. Shinozuka, M. S., and Levy, R., "Digital Generation of Alongwind Velocity Field," *J. Engineering Mechanics Div.,* Proc. ASCE 103 (EM-4), Proc. Paper 13159, Aug. 1977, pp. 689-700.

Table 1. Gravity and wind loading contributions to gain reduction

Source	Gravity loading[a]	Wind loading	
		Steady wind	Gust wind
A. Deformation type			
Backup structure deflection	Contr	Contr	Contr
Surface panel deflection	Contr	Contr	Contr
Subreflector offsets	Comp	Contr	Contr
B. Beam deviation type			
Backup structure pointing error	Calib	Corr	Contr
Alidade pointing error	Calib	Corr	Contr
Servo loop error	None	None	Contr

[a]Contr – Contributes to gain reduction
Comp – Compensated by subreflector repositioning
Calib – Calibration used to modify the commanded position
Corr – Corrected by programmed pattern search

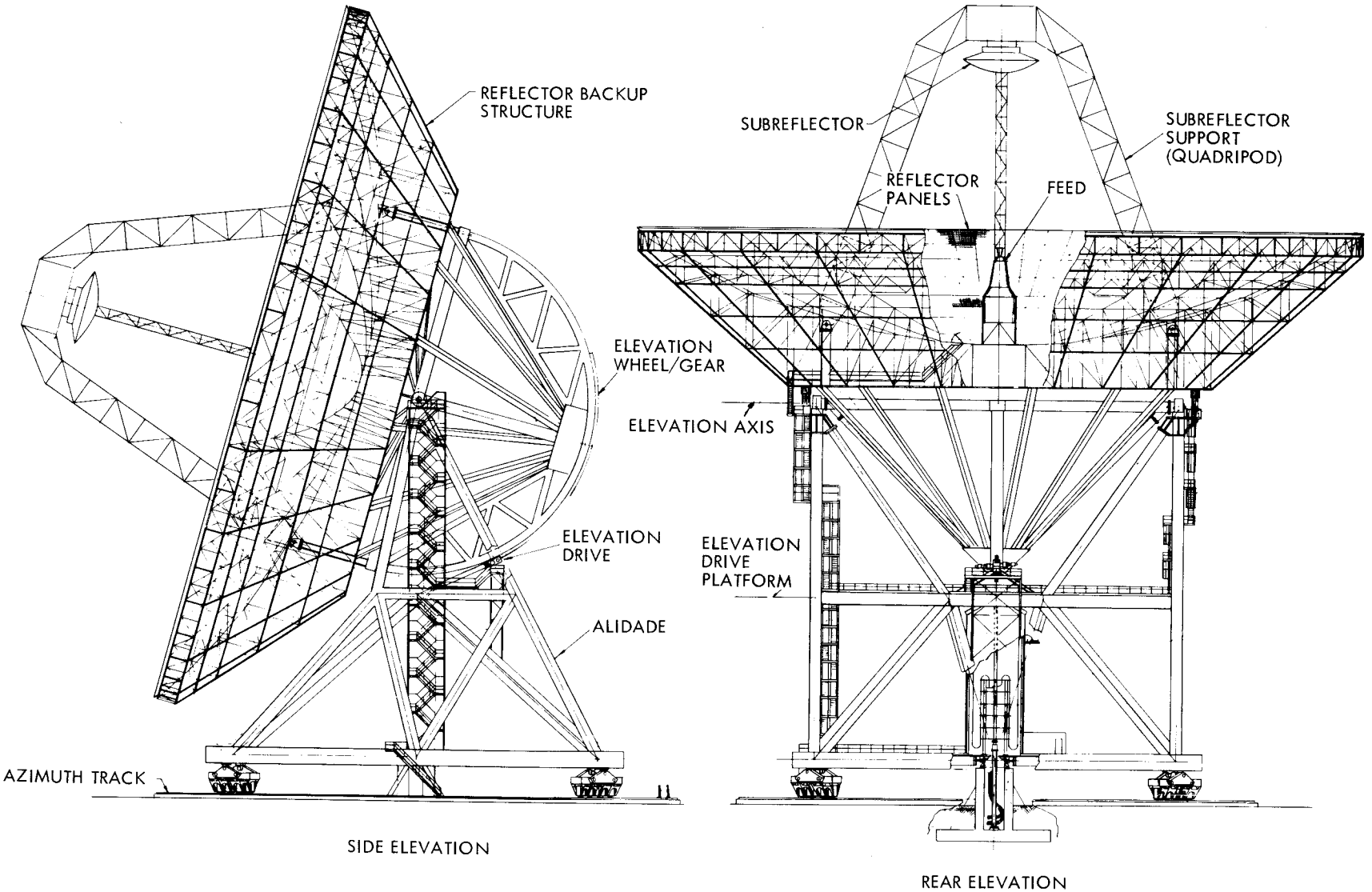

Fig. 1. Configuration of 100-m-diameter antenna system

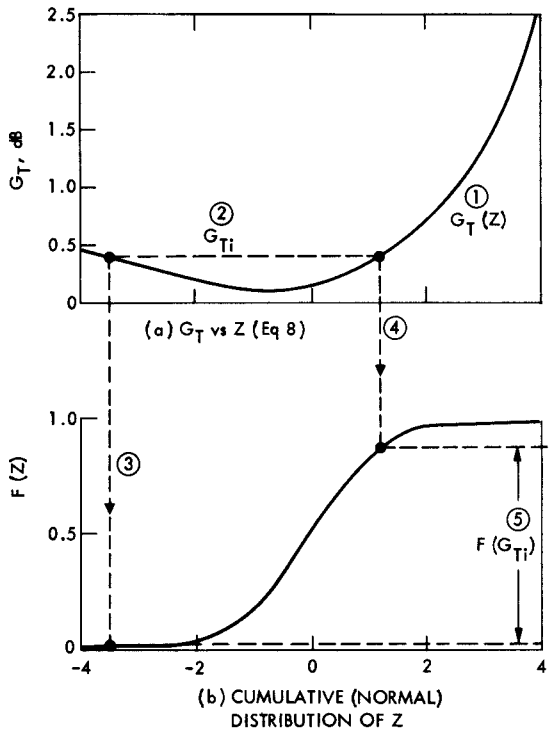

Fig. 2. Development of cumulative distribution of G_T

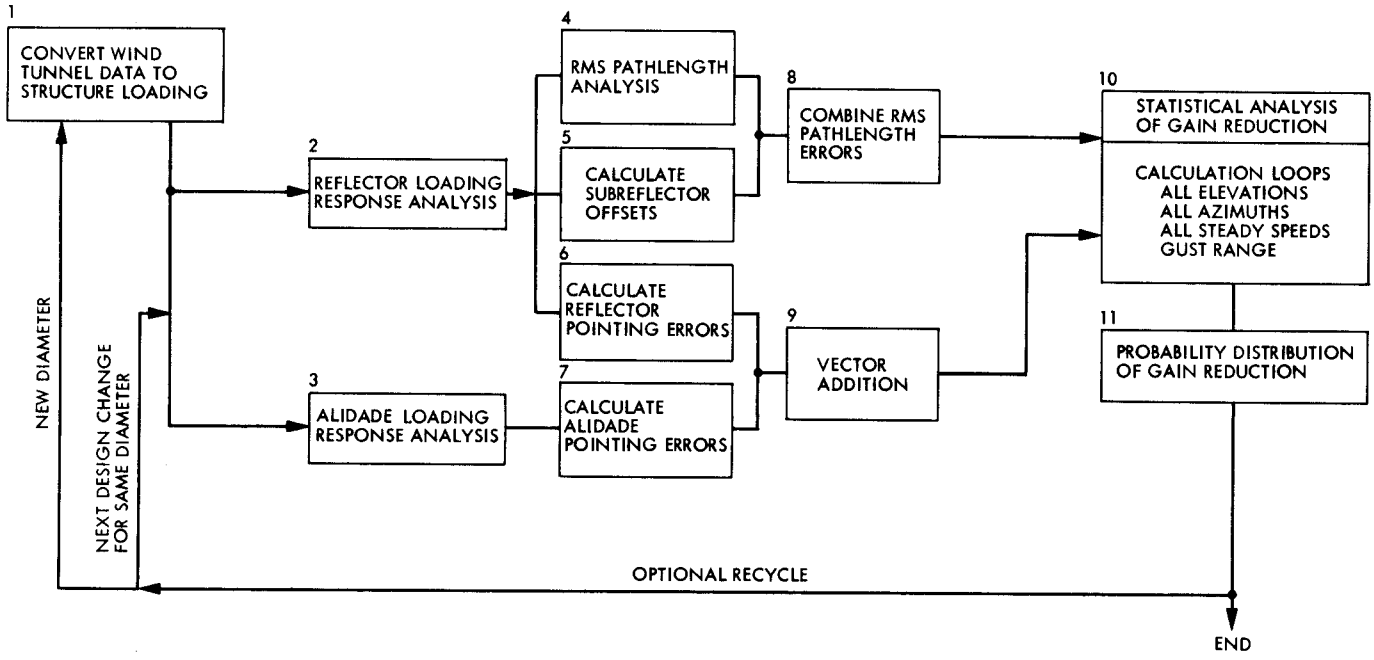

Fig. 3. Computational procedure

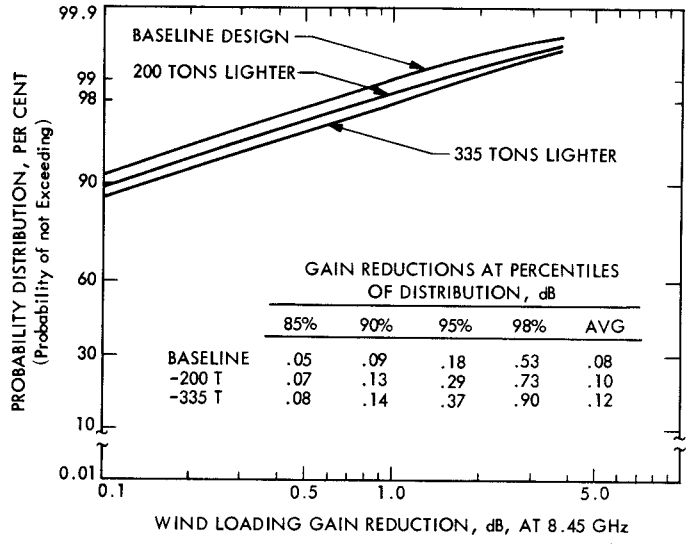

Fig. 4. Gain reduction for 100-m design variations